Biotechnology Research and Innovation (2019) 3, 22–37

Biotechnology Research & Innovation

http://www.journals.elsevier.com/biotechnology-research-and-innovation/

RESEARCH PAPER

Relevant aspects of the biosynthesis of porous aluminas using glycosides and carbohydrates as biological templates

Ángela B. Sifontes[a,*], Edward Ávila[b,*], Brenda Gutiérrez[a], Mine Rengifo[a], Andrea Mónaco[a], Yraida Díaz[a], Ligia Llovera[a]

[a] *Instituto Venezolano de Investigaciones Científicas, Centro de Química "Dr.Gabriel Chuchani", Laboratorio de Plasma Química y Nanomateriales, Caracas, Venezuela*
[b] *Instituto Venezolano de Investigaciones Científicas, Centro de Química "Dr. Gabriel Chuchani", Laboratorio de Síntesis y Caracterización de Nuevos Materiales, Caracas, Venezuela*

Received 25 October 2018; accepted 22 January 2019
Available online 10 April 2019

KEYWORDS
Alumina;
Biological templates;
Stevia rebaudiana;
Glucose

Abstract This research paper comparison of the use of biological templates obtained from steviol glycosides and glucose (monosaccharide) directed toward the synthesis of metal oxides. The results obtained shown the synthesis of aluminum oxides in an aqueous medium, using different green porogenic agents. The influences of the aging period and its impact on the alumina's porosity and phase transition were evaluated. The FTIR studies provided evidence of the surface modification of the aluminum oxide by carboxylate groups generated in the hydrolysis of diterpenic glycosides. The application of prolonged aging periods favored the production of η-alumina vs γ-alumina in the synthesis in which *Stevia rebaudiana* was used. The materials were characterized, using XRD, TGA, N_2 physical adsorption, FE-SEM, NMR, FTIR and TPD-NH_3. The TGA profiles indicate appreciable differences as to the yields achieved between samples prepared with the two biological templates (alumina–stevia up to 62%, alumina–glucose yields of 30%). The acidity obtained for the different aluminas synthesized by the use of biological templates showed a trend toward: glucose > stevia > sol–gel method/stevia, in the range of 0.994–0.485 mmol/g.

* Corresponding authors.
E-mails: angelasifontes@gmail.com (Á.B. Sifontes), edebavso@gmail.com (E. Ávila).

https://doi.org/10.1016/j.biori.2019.01.004

Introduction

During the last two decades, the biosynthesis of nanomaterials has received considerable attention due to the growing need to develop environmentally sociable technologies in material synthesis (Akhtar, Panwar, & Yun, 2013; Golinska et al., 2014). Among these, biosynthesis of nanoparticles from plants seems to be a very effective method in developing a rapid, clean and eco-friendly technology. *Stevia rebaudiana Bertoni*, commonly known as stevia, is a plant that synthesized in the leaves several compounds sweetening of high power and low caloric power. It is known that these sweeteners are diterpenic glycosides whose functional and sensory properties are superior to those of other high potency sweeteners, such as aspartame (Langle et al., 2015; Sadeghi, Mohammadzadeh, & Babakhani, 2015). Due to its characteristics and potential applications, stevia has been a very studied plant since the early twentieth century, and both its production and its trade have been increased with the improvement of the extraction and refining processes of its glycosides (Bujak et al., 2015; Kroyer, 2010; Langle et al., 2015; Sadeghi et al., 2015; Prakash et al., 2017; Upreti, Dubois, & Prakash, 2012). The research carried out to improve the performance in the processes of obtaining such glycosides has led to the optimization of aqueous extractions, now being simpler and cheaper than extractions with other solvents (Bujak et al., 2015; Kroyer, 2010; Langle et al., 2015; Sadeghi et al., 2015; Prakash et al., 2017; Upreti et al., 2012). This makes it particularly interesting when it comes to applications in the area of biosynthesis of nanomaterials. The development of simple procedures in aqueous phase is facilitated, being the well-known stevioside. Rebaudioside A (reb A) and stevioside (Fig. 1) are sweet ent-kaurene-type diterpenoid glycosides found in high concentration levels in the leaves of Stevia rebaudiana. The majority compounds of the organic extract, have been demonstrated to intervene as a biological template to generate porous nanostructures in the presence of

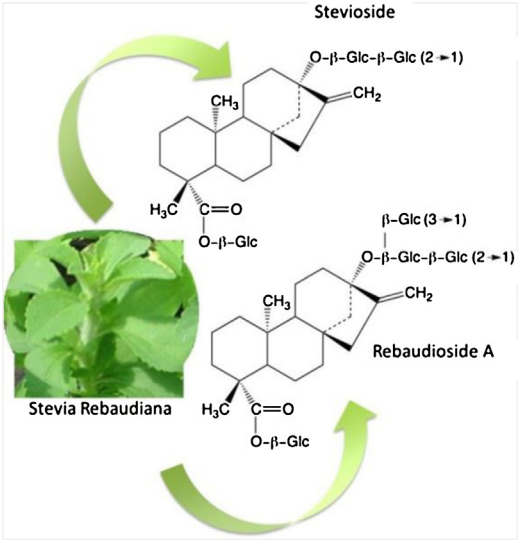

Figure 1 Main constituents of the aqueous extract of *Stevia rebaudiana*.

an inorganic precursor (Rodríguez, Sifontes, Méndez, Díaz, et al., 2013; Rodríguez, Sifontes, Méndez, Cañizalez, et al., 2013; Sifontes et al., 2013, 2015).

Structurally, stevioside (13-[2-Oβ-D-glucopyranosyl-a-glucopyranosyl)oxy]kaur-16-en-19-oic-acid-β-D-glucopyranosyl ester) is a glycoside with a glucosyl and a sophorosyl residue attached to the aglycone steviol, which has a cyclopentanonhydrophenanthrene skeleton (Bujak et al., 2015; Kroyer, 2010; Langle et al., 2015; Prakash et al., 2017; Sadeghi et al., 2015; Upreti et al., 2012). In aqueous solution stevioside is remarkable stable over a wide range of pH and temperature particularly, in the presence of different organic acids such as: acetic acid, citric acid, tartaric acid and phosphoric acid (Kroyer, 2010). These characteristics favor its use in the synthesis of nanometric metal oxides with a wide spectrum of applications in different scientific and industrial areas. Particularly aluminum oxide is highlighted (ceramic aluminas), materials that are frequently used as abrasives, thermal insulators, refractories, catalytic supports, and biomedical materials (prosthesis and implants) (Kim, Kim, Kim, & Yi, 2005; Martín & Weaver, 1993; Niesz, Yang, & Somorjai, 2005; Xiao et al., 2006). In the majority of countries alumina production (metallurgical grade), is carried out through the Bayer process (Burkin, 1987; Toro et al., 2001) for obtaining metallic aluminum. Another small part of the alumina is treated for purification, through a chemical process and a subsequent heat treatment (calcination) where generated different types, which can be employed depending on the degree of purity and the particle size in the ceramic industry (Burkin, 1987; Toro et al., 2001). However, all these processes involve high production costs, especially those associated with the removal of the sodium content which appears in the form of oxide as Na_2O. It adversely affects the electrical performance of ceramic aluminas. Also, during cooking beta alumina ($Na_2O{\cdot}11Al_2O_3$) can be formed, which reduces the mechanical strength, density and chemical resistance of the formed product (Burkin, 1987; Toro et al., 2001; Zyl et al., 1993).

Several studies have shown that ceramic grade alumina can be produced through different methods using analytical grade precursors (frequently aluminum alkoxides, aluminum monohydroxides (AlOOH), among others) but this is generally quite expensive.

Recently, the synthesis of aluminas by the sol–gel method of the alkoxides, has been developed for the preparation of simple and mixed oxides, being indicated as a technique that allows to improve the control of the textural properties of these materials and in particular, they are obtained solids with high surface area, an important attribute in materials with catalytic applications and adsorbents (Brinke & Scherer, 1990; Livage, Henry, & Sanchez, 1988; Park, Tadd, Zubris, & Tannenbaum, 2005).

However, its use has as limitations the requirement of a strict control of the conditions of synthesis and the application of complex post-preparation treatments (Brinke & Scherer, 1990; Livage et al., 1988; Park et al., 2005). In addition, this method of synthesis has presented as the main drawback the rapid hydrolysis of aluminum precursors in aqueous medium, which tend to form lamellar hydrated hydroxides in the presence of surfactant molecules (Kim

et al., 2005; Márquez et al., 2005; Toro et al., 2001; Xiao et al., 2006; Yoldas, 1975). Preventing the formation of lamellar aluminas is currently a challenge in the preparation chemistry of high surface area transition aluminas, particularly mesoporous aluminas (Kim et al., 2005; Márquez et al., 2005; Toro et al., 2001; Xiao et al., 2006; Yoldas, 1975). This tendency is even more evident when conventional preparative methodologies are used, probably due to the stabilization, in the course of the process, of anisotropic particles that are precursors of phases analogous to boehmite (Kim et al., 2005; Xiao et al., 2006; Yoldas, 1975). Aluminum alkoxide is obtained from a reaction between metallic aluminum and alcohol groups.

Hydrolysis of aluminum alkoxides will produce aluminum hydroxide, which can be transformed after heat treatment into Al_2O_3 powder (Márquez et al., 2005; Park et al., 2005; Yoldas, 1975). The following equations (1–3) show the reactions of this method, where R is hydrocarbon radical.

$$Al + 3ROH \rightarrow Al(OR)_3 + 3/2\,H_2 \text{ (alkoxide formation)} \quad \text{(Ec.1)}$$

$$Al(OR)_3 + 3H_2O \rightarrow Al(OH)_3 + 3ROH \text{ (hydrolysis process)} \quad \text{(Ec.2)}$$

$$2Al(OH)_{3(s)} \rightarrow Al_2O_{3(s)} + 3H_2O_{(g)} \text{ (thermal process)} \quad \text{(Ec.3)}$$

Currently, aluminum alkoxides are used as clean precursors in sol–gel processes for obtaining their oxides (Márquez et al., 2005; Park et al., 2005; Yoldas, 1975). The complex reactions that occur involve hydrolysis and condensation to polymeric species. It is known that the alkoxides present a great instability in aqueous media, frequently requiring the use of complexes with bidentate binders (acetates, acetylacetonate, etc.) to eliminate these problems (Brian, 1965; Pinnavaia, Zhang, & Hick, 2003; Toro et al., 2001). The functional groups of these complexes, promote greater stability to the hydrolysis and condensation reactions. However, highly drastic acid conditions are necessary to favor the rupture of the such complexes. drastically acid conditions are those that will not allow further hydrolysis and condensation of the metallic ion or an incomplete hydrolysis that would lead to materials with a high organic matter content. these could cause difficulties for the formation of a continuous network of metal oxide (Burkin, 1987; Park et al., 2005; Pinnavaia et al., 2003). In recent years alternatives have been sought for the establishment of a simpler method for the control of the hydrolysis and condensation speeds in these processes with greater simplicity. Alternatives are also seeked for the possibility of the use of less polluting products, and reduction of cost and production time of the nanomaterial. An example of this possibility has been the use of carboxylic acids (HCA)—citric (from fruits), tartaric (present in plants and grapes) and lactic (generated during fermentation processes)—as pore-forming agents in the preparation of aluminas (Barron, 2014; Liu, Wang, Wang, & Zhang, 2006). These studies reached the conclusion that the synthesized materials had porous structures with a narrow pore-size distribution and surface areas that did not exceed 381 m^2/g. Depending on the carboxylic acid used, variations in morphology and textural characteristics were observed. It is important to mention that these acids are small molecules that cannot form micellar structures, but they could interact with the metal hydroxide (boehmite), and coordinate with it in a similar way to the formation of the complexes of aluminum ions in solution as shown in equation E.4 (Barron, 2014; Schilling et al., 2002).

$$\equiv Al\text{-}OH_2^+ + H_2\text{-}L^- \leftrightarrow \equiv Al\text{-}LH_2 + H_2O \quad \text{(Ec.4)}$$

L indicates ion HCA.

By this procedure, it has been shown that high surface area aluminas can be obtained, using simple, economical and less polluting synthesis routes, using organic agents of natural origin, and eliminating the use of surfactant molecules. In the development of these new synthesis routes, and consistent with principles of green chemistry, it has also been shown that *glucose* can be used as an excellent organic adjuvant agent in the formation of porous structures. Xiao et al. (2006) extended this methodology to alumina systems; managed to obtain mesoporous and amorphous aluminas with high surface area with a narrow pore-size distribution and an excellent thermal stability by the use of an aluminum alkoxide precursor. The preparation process and the properties of the aluminas synthesized by this procedure illustrates the combined use of glucose as a porogenic agent and an aqueous medium, using a simple synthesis route.

In general, "the organic compound used can act by controlling the hydrolysis of the aluminum alkoxide, if it contains in its structure active hydrogen atoms, hydroxyl groups, carboxyl, amide acids, imides, sulfonic acids, phenolics or ketoenol groups" (Davidson, 1965; Schilling et al., 2002; Toro et al., 2001). Examples of such substances are tribromoethanol, tri-chloro-tertbutanol, methyl pentynol, benzyl alcohol, glycerol, ethanolamine, salicylic acid and its esters, ascorbic acid, oligosaccharides such as sucrose, lactose, maltose and glucose. ''The compound obtained in the synthesis would be present under the formulation'' (Davidson, 1965):

$$(X_2AlO)(AlOX)p(AlX_2) \quad \text{(Ec.5)}$$

where "$p = 0$ and X could be a hydroxyl group or a residue of the controlling substance of the hydrolysis" (Davidson, 1965). Subsequently, if an excess of water is added, it will produce a value of $p > 1$ and facilitate the condensation of the aluminum-oxygen compound (Davidson, 1965; Schilling et al., 2002; Toro et al., 2001).

Recently, the aqueous extract of *Stevia Rebaudiana Bertoni* for the synthesis of porous metal oxides has been published (Rodríguez, Sifontes, Méndez, Díaz, et al., 2013; Rodríguez, Sifontes, Méndez, Cañizalez, et al., 2013; Sifontes et al., 2013, 2015). Steviol glycosides, the main constituents of *S. rebaudiana*, have demonstrated to be an authentic biological template in the synthesis of nanometer-scale materials. Observations on the structural formula of the glycosides present in the aqueous extract of *S. rebaudiana* indicate that the hydrophilic region of the molecule possesses dimensions that are comparable with the tetracyclic hydrophobic fragments. These molecules have the particularity of interaction of their hydrophilic portions with their hydrophobic fragments, and to achieve true supramolecular structures. these structures have the capability of assembling with inorganic species (Rodríguez, Sifontes, Méndez, Díaz, et al., 2013; Rodríguez, Sifontes, Méndez, Cañizalez, et al., 2013; Sifontes et al., 2013, 2015). These glycosides therefore have the possibility of preferentially interacting and forming laminar structures

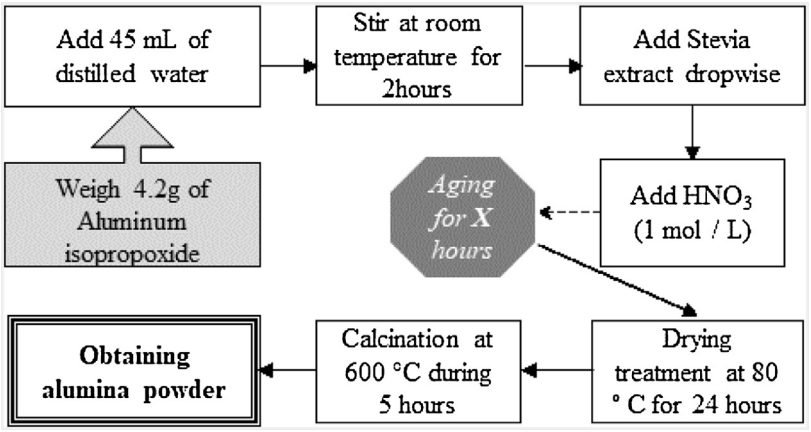

Figure 2 Schematic procedure for the synthesis of alumina using stevia template in an aqueous system.

with alternating layers, composed of both types of fragments. On the other hand, under these reaction conditions, in an aqueous system and the presence of isopropanol, the diterpenic glycoside molecules can be solvated. The glycoside residues and the tetracyclic molecular structure could be placed one on top of the other forming an intramolecular cavity (Rodríguez, Sifontes, Méndez, Díaz, et al., 2013; Rodríguez, Sifontes, Méndez, Cañizalez, et al., 2013; Sifontes et al., 2013, 2015), which could facilitate the formation of the porous structure. Subsequently, the interaction of the formed structure with the inorganic precursor will allow the formation of a hybrid compound. The obtention of the solid is finally completed by eliminating the organic fraction or ''template'' through a heat treatment: drying at 100 °C and subsequent calcination at high temperatures.

This experimental study is based on comparison of the use of biological templates obtained from steviol glycosides and glucose (monosaccharide) directed toward the synthesis of metal oxides. Particularly, results are shown regarding the synthesis of aluminum oxides in an aqueous medium, using different green porogenic agents. Many unanswered questions related to the mechanisms involved and obtaining the final product are discussed. From the technological point of view, the discussion of these items is of interest as related to the development of materials with catalytic applications. In this sense, the acidic properties of the aluminas was studied.

On the other hand, although it is true, that the synthesis of mesoporous aluminas using the extract of Stevia Rebaudiana has been evaluated, the possible modification of the metal oxide surfaces by this organic environment has not been extensively studied, neither the effect of the variation of synthesis parameters, particularly the aging period and its impact on the alumina's porosity and phase transition.

Materials and methods

Aluminas were prepared according to procedure reported by Rodríguez. It was modified extending the aging period to 48 h (Rodriguez et al., 2013). In this methodology, aluminum isopropoxide, $Al(OC_3H_7)_3$ (Sigma-Aldrich) was hydrolyzed by adding it into excess deionized water (75 mole water/1 mole Al^{3+}) under continuous stirring for 2 h (Scheme, Fig. 2). In a second step, *S. rebaudiana* extract was added and stirred in the precursor solution. After standing for 48 h (18 h and 6 h were also evaluated), the synthesized solids were subjected to a thermal treatment to evaluate the effect of temperature on their crystallinity, textural properties and morphology. The mixtures were heated at 80 °C in open air to remove water and all other volatiles. The dry solids were calcined at 600 for 6 h and 1000 °C for 6 h to remove the template employing heating and a cooling rate of 5 °C/min. Two samples were prepared by the sol–gel method, employing the extract of *S. rebaudiana* and a reference wuth no molecules of estevioside (Scheme, Fig. 3). The sol–gel reaction consisted of the transformation of the aluminum oxy-hydroxide—AlO(OH)—particles into the aluminum oxide network by a dehydration process (Raybaud et al., 2001; Urretavizcaya, Cavalieri, Porto, & Sanz, 1998). The alumina suspensions were then dried in an oven at 80 °C and calcined at 600 °C employing heating and a cooling rate of 5 °C/min.

The Al_2O_3 materials were prepared using glucose as the biotemplate according the following procedure (Xiao et al., 2006): ''4.2 g of aluminum i-propoxide and 3.6 g of glucose were dissolved in 54 mL of distilled water; the resultant solution was stirred at room temperature for 30 min. The molar ratio of Al^{3+}:glucose:H_2O in the solution was 1:1:75. A diluted aqueous nitric acid (10 wt.%) solution was subsequently added dropwise to adjust the pH to 5''. After standing for 5 h, the mixture was heated at 100 °C in open air, to remove water and all other volatiles. The resulted solid was then calcined at 600 °C for 6 h, to remove the template.

Table 1 shows the identification of synthesized solids, the biological template used, and the respective conditions of temperature and aging time. The prepared solids were characterized using a Siemens D-5000 X-ray diffractometer (XRD), using CuKα radiation in the 2θ range between 5° and 70° in order to examine their possible crystalline structure. The surface area was determined by nitrogen adsorption at −196 °C, in a Micromeritics ASAP 2010 equipment and was calculated following the Brunauer–Emmett–Teller (BET) (Brunauer et al., 1938; De Boer, 1958; Tilley & Eggleton, 1996) method. The pore size distribution was obtained according to the Barret–Joyner–Halenda method (BJH). Observations by scanning electron microscopy with

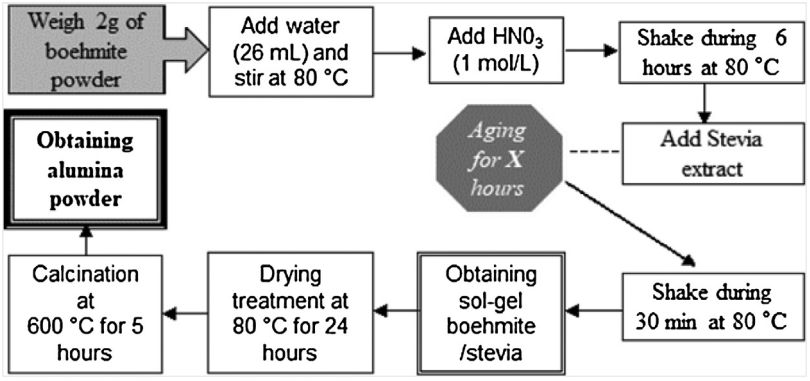

Figure 3 Schematic procedure for the synthesis of alumina by the stevia-sol gel process.

Table 1 Samples identification.

Precursor	Sample No	Temperature °C	Aging time (h)
Isopropoxide	AS-1	600	48
aluminum/stevia	AS-2	1000	48
Boehmite gel/stevia	ABS-600	600	48
Boehmite	AB-600	600	48
Isopropoxide aluminum/stevia	AS-3	600	18
Isopropoxide aluminum/stevia	AS-4	600	6
Isopropoxide aluminum/glucose	AG-1	600	48
Isopropoxide aluminum/glucose	AG-2	600	18
Isopropoxide aluminum/glucose	AG-3	600	6

field emission (FE-SEM) were performed on a Quanta 250 FEG instrument with an accelerating voltage of 30 kV. The infrared spectra with Fourier Transform (FTIR) were obtained using a Perkin Elmer Spectrum RX1 equipment.

Thermal analysis were carried out in the temperature range ambient −1000 °C at a heating rate of 10 °C/min and under air flow using a simultaneous thermal analyzer TGA/DSC, model Stare System, by Mettler Toledo, to trace changes in physical and chemical properties of the synthesized materials, as a function of increasing temperature. Thermal analysis is of primary importance for the understanding of the ways in which the modification of alumina surface is related to aging time, temperature changes and the changes in the stevia glucose biological template.

^{27}Al MAS-NMR (magic angle spinning-nuclear magnetic resonance) spectra were recorded in a Bruker Avance 300 MHz spectrometer at 78.172 MHz (7.0463 T magnetic field).

Quantitative determination of the acid sites of γ-alumina was performed by the temperature-programmed desorption of ammonia (NH_3-TPD) using an Autochem II Chemisorption Analyzer Micromeritics, with the Autochem II 2920 V3.02 SOFTWARE.

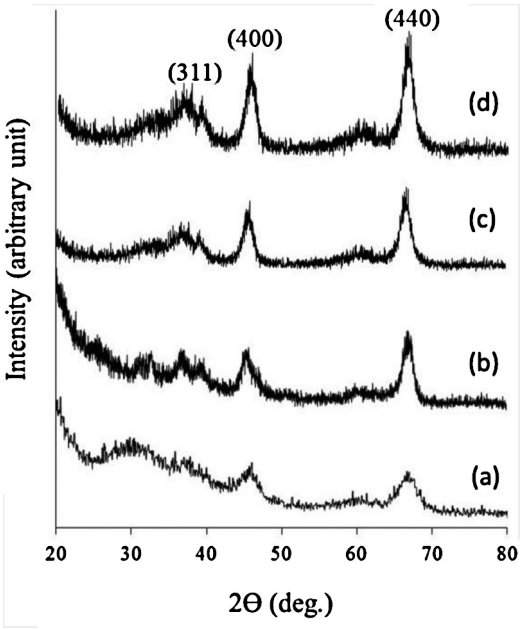

Figure 4 XRD patterns for aluminas synthesized employing stevia as biological template: (a) AS-1, (b) AS-2, (c) AB-600, and (d) ABS-600.

Results and discussions

The crystalline phase of calcined alumina for solid obtained during a 48-h period was confirmed by XRD. In principle, a study was carried out by XRD for the identification of the synthesized solids. Figs. 4 and 5, shows the diffractograms of the materials calcined where the characteristic peaks of aluminum oxide are observed. The reflections at 2θ of 38°, 45° and 67°, were attributed to the d_{311}, d_{400} and d_{440} planes of the gamma alumina phase (Barron, 2014; Martín & Weaver,

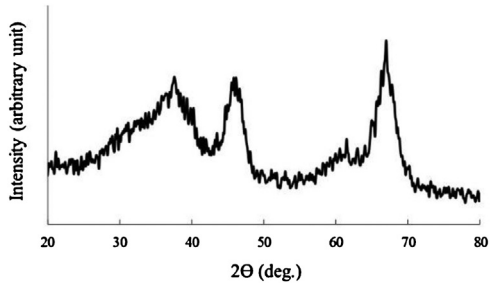

Figure 5 XRD patterns for alumina synthesized employing glucose as the biological template.

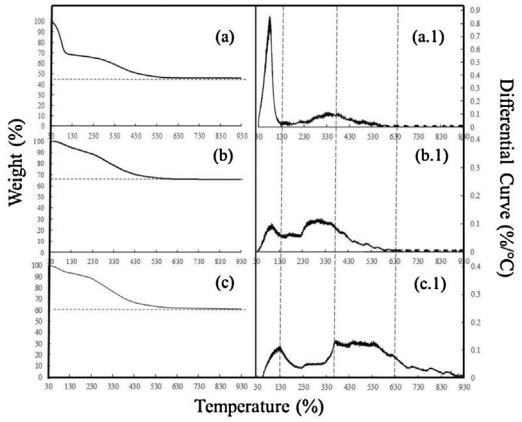

Figure 6 TGA and DTGA profiles of as-synthesized alumina prepared with the stevia template: (a) aging 6 h, (b)18 h, and (c) 48 h.

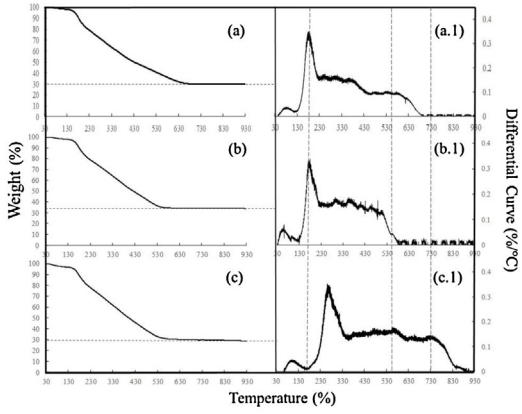

Figure 7 TGA and DTGA profiles of as-synthesized alumina prepared with glucose template: (a) aging 6 h, (b)18 h, and (c) 48 h.

1993; Márquez et al., 2005; Maciver, Tobin, & Barth, 1963; Maciver, Wilmot, & Bridges, 1964; Niesz et al., 2005; Park et al., 2005; Zhou & Snyder, 1991;). The widening of the Bragg peaks in the diffractograms can be attributed to the small particle size of the obtained solids.

The thermal stability and the influence of the aging period in obtaining the final product was studied by thermal gravimetric analysis (TGA) from ambient up 930 °C. Figs. 6 and 7 illustrates thermal gravimetric profiles of synthesized aluminas whith stevia and glucose, applying aging periods of 6, 18 and 48 h. The first weight loss corresponds to physically adsorbed water and alcohol. The second weight loss is attributed to the starting point of phase transformation from aluminum hydroxide, dehydration/dehydroxylation to an active alumina phase by condensation of adjacent surface or internal hydroxyl groups (220–600 °C), and the elimination of organic molecules. The phase transformation from aluminum hydroxide to active alumina began at 240 °C, and the active alumina phase was retained up to 550 °C for both biological templates. The aluminas prepared using the stevia extract present considerable differences when long periods of aging are established (until the reach 48 of hours). Probably, some steviosides or other diterpenic glycosides are coordinated with aluminum hydroxide. However, other alumina particles are assembled in to large aggregates and crystallized in the composite during drying. These large aggregates might result in the formation of additional large mesopores in the calcined sample. On the other hand, one can infer that some of these organic groups could be strongly retained on the surface of the alumina, up to temperatures above 550 °C. The possible differences between the existing interactions between the biological template and the inorganic precursors are reflected in the total mass loss of both materials, being of 70% in the case of glucose and 38% for aluminas prepared with stevia. This fact has a strong impact for future technological applications because the low yield in the synthesis limits its feasibility for industrial production. Comparing it with the aqueous system, a significant decrease in yield (17%) is observed with the material obtained through the sol–gel method (Fig. 8).

The coordination of Al atoms to the active alumina as dependent on preparation conditions was investigated by ^{27}Al MAS NMR. The ^{27}A1 MAS-NMR spectra of the AS-1(template stevia) and AG-1 (template glucose) samples are given in Fig. 9. The spectra are formed by two components at ~5 and 65 ppm, which correspond to octa- and tetrahedral-Al, and their satellite spinning sidebands spaced at ~40-ppm intervals (spinning rate of the sample expressed as ppm) (John et al., 1983; Meinhold et al., 1993; Mizushima et al., 1993). As shown in Fig. 9, the ratio of Al^{VI} to Al^{IV} for calcinated samples of alumina AS-1 and AG-1 is 1.6 and 2.9 respectively. In the literature, percentage of –coordinated Al present is reported to be (75 ± 4) % Al^{VI} in γ-alumina and (65 ± 4) % Al^{VI} in η-alumina (John et al., 1983; Meinhold et al., 1993; Mizushima et al., 1993). Namely, the Al^{VI}/Al^{IV} value is 2.4–3.8 in γ-alumina and 1.6–2.3 in η-alumina. For AG-1 the chemical shift values of tetra- and octahedral components are similar to those reported by Muller et al. (1986) and Komarneni et al. (1985), respectively, for a commercial sample and for a γ-Al_2O_3 obtained from boehmite. γ- and η-Al_2O_3 structures are frequently obtained with X-ray powder diffraction patterns, and show broad reflections that correspond to cation-defective spinels (Bendig & Scamehorn, 1978; Souza, Souza, & Toledo, 2000). This is concordant with results shown in Fig. 4. The structure of γ-$A1_2O_3$ and η-$A1_2O_3$ can be derived from a cubic closest packing (CCP) array of oxygens in which one-eighth of the tetrahedral interstices and half of the octahedral interstices are occupied by the cation. All spinels contain two differing cations or at least two different valences of the same cations in the ratio of 2:1 (Bendig & Scamehorn, 1978; Maciver et al., 1963; Souza

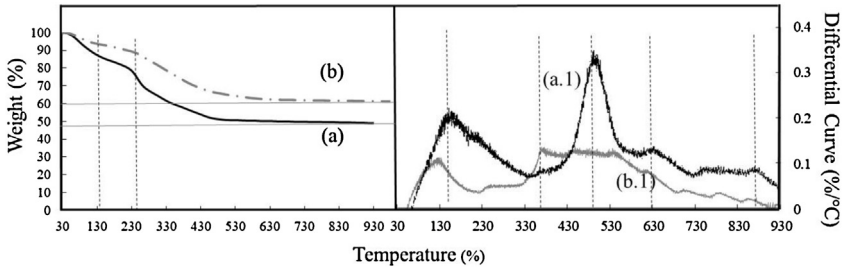

Figure 8 TGA and DTGA profiles of as-synthesized alumina prepared with the stevia template: (a) aqueous system and (b) sol–gel.

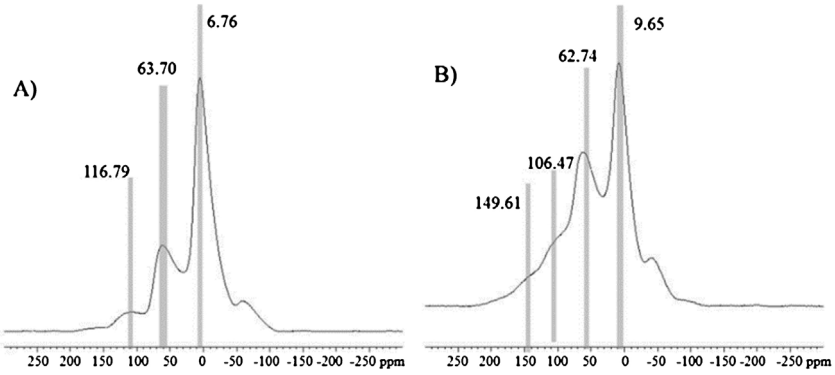

Figure 9 ^{27}Al MAS NMR spectra corresponding to alumina synthesized with (a) glucose and (b) stevia.

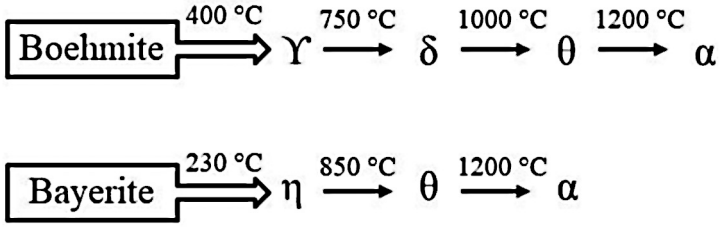

Figure 10 Thermal decomposition pathways of gibbsite, and boehmite adapted from Shirai et al. (2009).

et al., 2000; Pecharromán, Sobrados, Iglesias, Gonzalez, & Sanz, 1999). This is a consequence of the dehydroxylation reactions where the skeleton of the parent material is preserved while OH– groups are eliminated. If the oxygen network of the precursor is close to a face-centered cubic (fcc) structure (boehmite and bayerite), heating treatments produce spinel-like materials (Maciver et al., 1963). The ideal structure of these phases belongs to space group Fd3m, but their real structure seems to be tetragonally distorted. Distortions are different in both phases (γ- and η-) and they have been associated with differences in cation ordering. On these bases, tetrahedral Al fractions (frAl-tet) in γ-Al_2O_3 will be 0.25, which is experimentally confirmed (Fig. 9A). From this fact, the γ-Al_2O_3 can be considered as a defect spinel in which cation vacancies are considerably ordered (Yoldas, 1973). In alumina synthesized with the stevia extract, the frAl-Tet values was 0.39, probably indicating a higher degree of disorder in the cation vacancy disposition.

The aluminas synthesized using the same methodology and different biological template show different phase transitions. ''The formation of η-alumina was attributed to the extension of the aging to 48 hours. At room temperature, hydrolysis of aluminum alkoxides followed by a period of aging, as demonstrated in the results of the experiences made by Yoldas'' (Shirai et al., 2009; Yoldas, 1973), the bayerite (precursor of the η-alumina) can be present. It is well known that the formation of transition aluminas as well as part of their structural properties depend on the type of the starting aluminum hydroxide (Fig. 10). When the hydrolysis of aluminum alkoxides is performed by cold water the resultant monohydroxide is largely amorphous and converts to trihydroxide (bayerite) in its mother liquor at room temperature (Ec.6). The conversion to bayerite occurs through a dissolution–recrystallisation process of the amorphous phase. Differently, hydrolysis of aluminum alkoxides with hot water results in the formation of crystalline monohydroxide, boehmite, which is relatively unaffected by aging (Maciver et al., 1963, 1964; Yoldas, 1973; Zhou & Snyder, 1991). In general, η-Al_2O_3 may be produced from two routes: (i) from bayerite; (ii) from gelatinous boehmite. Gelatinous

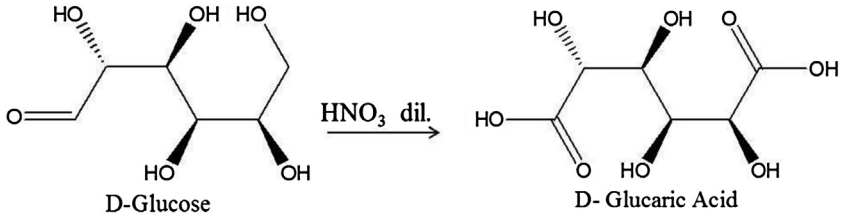

Figure 11 Oxidation of glucose in dilute nitric acid.

boehmite is a synonymous of pseudoboehmite; it is constituted by a linear polymer of the – (AlOOH) – group (Bendig & Scamehorn, 1978; Digne, Sautet, Raybaud, Toulhoat, & Artacho, 2002; Maciver et al., 1963, 1964; Mishra et al., 2000; Lippens & Boer, 1964):

$$\text{alkoxide} + H_2O \rightarrow \text{amorphous alumina} \rightarrow (\text{aging h}) \rightarrow \text{pseudoboehmite} \rightarrow (\text{aging h}) \rightarrow \text{bayerite} + \text{alcohols} \quad \text{(Ec.6)}$$

Consecutively, bayerite decomposition to the η-phase is produced, involving elimination of OH groups [2 $Al(OH)_3 \rightarrow \eta A1_2O_3 + 3H_2O$]. It is important to mention that thermal transformations η-θ-α alumina are not detected by TGA. In these transformations, a small amount of energy is involved and no weight loss is produced. Under synthesis conditions bayerite is thus formed by the dissolution of the pseudoboehmite and recrystallization in the presence of a large molar excess of water. It is to expect that a small amount of bayerite present during synthesis is converted to boehmite. A competition between a partial dehydration of bayerite into boehmite and a total dehydration into η-alumina could occurs at higher temperature. A quantitative experimental study of this phenomena can be found in the work of Zhou and Snyder (Maciver et al., 1963). Starting from pure bayerite, they follow the calcination process by XRD and DTA. At about 540 K, they observed a mixture of bayerite and boehmite, leading at about 590 K, to a mixture of η-alumina and boehmite. On the other hand, ''Lippens and de Boer have also mentioned that it is impossible to obtain pure η-alumina from bayerite'' (Digne et al., 2002). Indeed, at the early stage of the calcination, a small amount of bayerite is converted into boehmite (Tonkovic & Bilinski, 1994).

The TGA profiles reveal appreciable differences for the sample prepared with glucose, obtaining a different phase transition despite the employment of a long period of aging. In this regard, it is concluded that the protection of the precursor particles by molecules that arise from the organic environment and which are anchored strongly on their surface prevent structural changes in the precursor, aluminum hydroxide, generated as a product of the alcohol hydrolysis. The use of glucose in the synthesis is attributed to the main chemical characteristic of carbohydrates: the presence of a functional group of the carbonyl type (aldehyde or ketone) and several hydroxyl groups. It is important to note that aldoses (with aldehydes as a functional group) can be oxidized in dilute acid medium (Fig. 11, synthesis medium) (Donald, 2000; Haworth & Jones, 1944; Sabari et al., 2004; Stanek, Kocourek, & Pacak, 1963) to give derivatives of carboxylic acids.

The procedure proposed by Xiao et al. (2006), a carboxylic acid (HCA) is certainly formed under synthesis conditions, acting as an organic agent and generates coordination interaction between boehmite colloids and HCA molecules. It is known that HCA are good complexing agents for aluminum in aqueous solution with two possible coordination modes: monodentate or bridging bidentate (Barron, 2014).

A FTIR study was carried on synthesized samples using different calcination temperatures (Fig. 12(a) and (b)), methods of treatment (Fig. 12(c) and (d)); and different biological templates at different times of aging (Fig. 13(I and II)). These spectra were characterized by the presence of a broad band between 900 and 400 cm^{-1}, which is attributed to the vibrations of the link Al=O (Kim et al., 2005; Khaleel & Klabunde, 2002; Morterra et al., 1977; Panasyuk et al., 2011). These results are consistent with XRD analysis, where the aluminum oxide was identified (Fig. 4). For the sample AS-2 additional vibrations are observed around 824 and 660 cm^{-1}, possibly associated with the presence of octahedral AlO_6 structures, which may indicate the beginning of a phase transition to α-alumina (Kim et al., 2005; Khaleel & Klabunde, 2002; Morterra et al., 1977; Panasyuk et al., 2011). It is important to note that in the calcined samples AS-1 (Fig. 12(a)) and AS-2 (Fig. 12(b)), several signals are observed in the region of 1737, 1637, 1400 and 1381 cm^{-1}, which seem to indicate that the surface of alumina could also be covered with carboxylate groups (Kim et al., 2005; Khaleel & Klabunde, 2002; Morterra et al., 1977; Panasyuk et al., 2011). These signals or peaks are attributed to the chemical species (carboxylate groups) that are generated from the acid hydrolysis of the steviosides (diterpene glycosides), steviol and isosteviol. These species could interact with intermediaries of the reaction of the alkoxides, the metallic monohydroxide or trihydroxide, and coordinate with aluminum species in solution. In Fig. 13, it can be seen that these carboxylate groups prevail at 1000 °C. They protect the inorganic structure and avoid its aggregation or sintering, and prevent subsequent phase changes and the substantial modification of textural properties and morphology of the structure. Concurrently, different types of carbonate formation (monodentate, bidentate and bridged) can occur on metal oxide surface, depending upon the geometry of the coordination of aluminum. Alumina is an amphoteric oxide and it, not only possesses acidic sites, but also basic sites. CO_2 adsorption on basic sites usually forms carbonate species, and alternatively, CO_2 adsorption on acidic sites forms bicarbonate species. The CO_2 adsorption on metal oxide surfaces

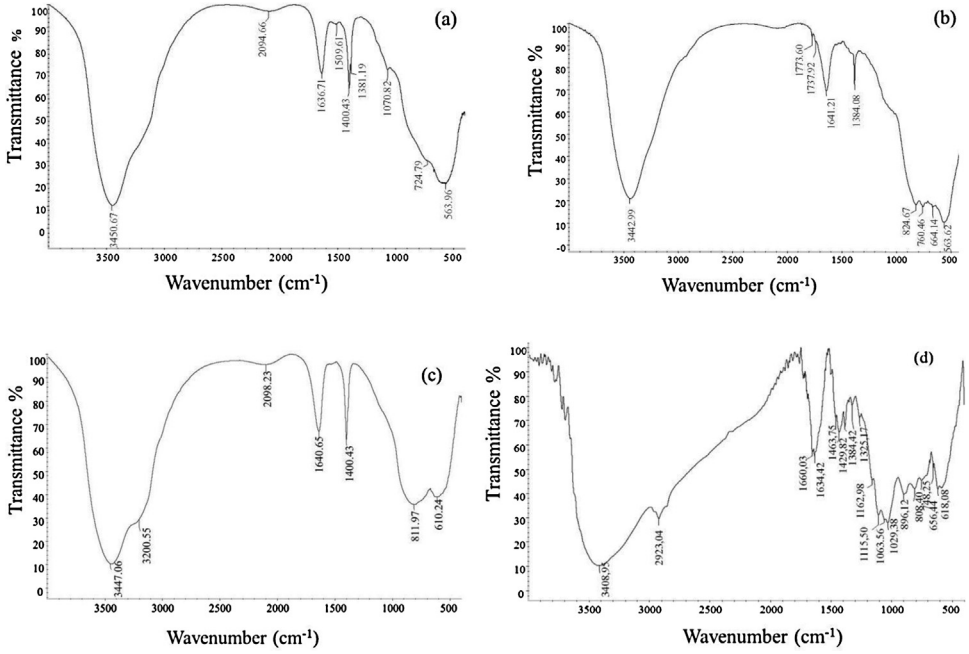

Figure 12 FTIR analysis of the samples: (a) AS-1 (600 °C), (b) AS-2 (1000 °C), (c) AB-600, and (d) ABS-600.

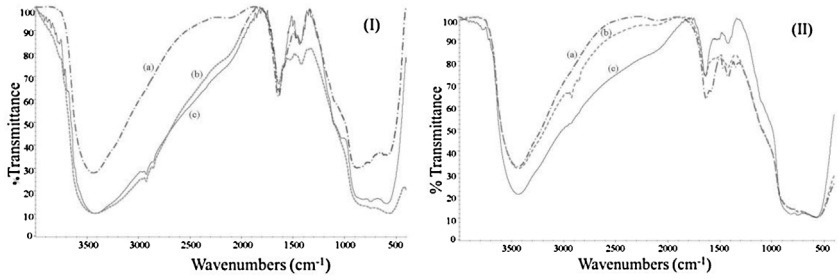

Figure 13 Comparative FTIR analysis of samples prepared at 1000 °C during aging periods of (a) 6, (b) 18 and 48 h, employing as biological template, (I) stevia extract and (II) glucose.

Table 2 Comparative experimental vibrational frequencies for synthesized aluminas AS-1, AS-2 and ABS-600

Adsorbed species	Vibrational mode	As-1(cm^{-1})	SamplesAs-2(cm^{-1})	Bs-600 (cm^{-1})	References
Bicarbonate					
	ν_2(O–C–O)	1636	1641	1640.65	1620–1670
	ν_3(O–C–O)s	1443	–	1463, 1429, 1500	1396–1500
	δ_4(O–C–O)	–	–	–	1220–1270
Carbonate					
Monodentate					
	ν_1(C–O)s	1071	–	1063	1010–1070
	ν_3(O–C–O)s	1381	1384	1384	1360–1390
	ν_3(O–C–O)a	1400, 1500	–	1463, 1429, 1500	1400–1590
Bidentate					
	ν_1(C–O)s				1020
	ν_3(O–C–O)s	–	–	1162, 1325	1140–1360
	ν_3(O–C–O)a	1636	1641	1660, 1634	1530–1670
Bridged					
	ν_1(C–O)s	–	–	–	1035
	ν_3(O–C–O)s	–	–	–	1230–1200
	ν_3(O–C–O)a	–	–	1660	1650–1710

under dry condition, results in the formation of adsorbed carbonates, bicarbonates, and formates as well as bent CO_2 species. In Fig. 13, the presence of intense bands is observed at 1642, 1443, and 1226 cm^{-1}, which could be attributed to bicarbonate species formation [60–66]. It is important to note that vibrational bands situated below 830 cm^{-1} are associated to Al=O vibrations, could also correspond to the vibrations of $\delta(CO_2)$, $\delta(OCO)$, $\nu(OC\text{-}(OH))$ and ν(H torsion) bicarbonate species (Baltrusaitis et al., 2006; Galhotra, 2010; Hoggan et al., 1994; Iordan et al., 2004; Ramis et al., 1991; Shek et al., 1997; Yúnes, 2000). For the purpose of illustration literature references on the vibrational frequencies for carbonate/bicarbonate formation in different aluminum materials are shown in Table 2. The possible bicarbonate species observed could be generated between CO_2 pre-adsorbed on the surface of the metal-oxide and the intermolecular proton transfer by the neighboring hydroxyl groups of aluminum sites. The underlying peaks at 1132, 1384 and 1508 cm^{-1} are respectively associated with the monodentate form of carbonate, for the ν(O–C–O)a, ν(O–C–O)s and ν(C–O)s modes (Baltrusaitis et al., 2006; Galhotra, 2010; Hoggan et al., 1994; Iordan et al., 2004; Ramis et al., 1991; Shek et al., 1997; Yúnes, 2000). They could also be shown in spectra of samples as of Fig. 13. Peaks associated to the modes corresponding to bidentate carbonate and bridged carbonate formation were not observed. It is interesting to mention that, differences in the surface chemistry of the transition aluminas as well as the Al^{3+} coordination of metal oxide, determines the presence or absence of these chemical species. For example, Al^{3+} coordination in octahedral coordination preferentially locates basic O^{2-} ions toward the surface which leads to carbonate formation. The same considerations are established for sample (d), ABS, where the identification of some bands at 1633, 1587, 1470, 1418, 1345 and 1340 cm^{-1}, corresponds to carboxylate groups. The spectra corresponding to the standard alumina, synthesized without the organic agent, prepared through the thermal treatment of boehmite, show two bands of strong intensity at 1640 and 1400 cm^{-1}, They are attributed to bicarbonate species (Baltrusaitis et al., 2006; Galhotra, 2010; Hoggan et al., 1994; Iordan et al., 2004; Kim et al., 2008; Ramis et al., 1991; Shek et al., 1997; Yúnes, 2000). Conversely, peaks associated to the modes corresponding to bidentate carbonate and bridged carbonate formation the peaks were not observed.

For both biological templates, a comparative analysis at different aging times show the possible modification of the alumina surface by carboxylate groups which become evident at temperatures of 1000 °C. This can provide an effective barrier that avoids sinterization and the decrease of their surface area and also increasing their thermal stability. The presence of functional groups on alumina surfaces may significantly expand applications of these materials, particularly applications in the medical field. The presence of carboxyl groups on the surface of aluminas alters its surface charge, and this charge affects surface bioactivity.

Isotherms of nitrogen adsorption at liquid nitrogen temperature (77.3 K) on the (a)AS-1, (b) AS-2, (c)ABS-600, (d) BS-600 samples are shown in Figs. 14–16. The pore size distributions were obtained from the adsorption branch of the N_2 isotherm by means of a BJH treatment. From this analysis, it can be noted that the AS-1 and AS-2 were characterized by a pore size with about 95% of the pore volume being in pores of 2–21 nm radius. *Eta*-alumina, on the other hand, exhibited a somewhat bimodal pore distribution with 56% of the pore volume in pores less than 8 nm radius. These two types of pore-size distributions appear to be typical of the respective aluminas and have been noted and discussed by Lippins (Maciver et al., 1963). As can be seen in Fig. 14, the isotherm A1 corresponding to the sample calcined at 600 °C presented a concordant behavior with a type IV isotherm (IUPAC classification) (De Boer, 1958; Galhotra, 2010; Harkins & Jura, 1943; Gregg & Sing, 1991; Shana et al., 2003; Yúnes, 2000), corresponding

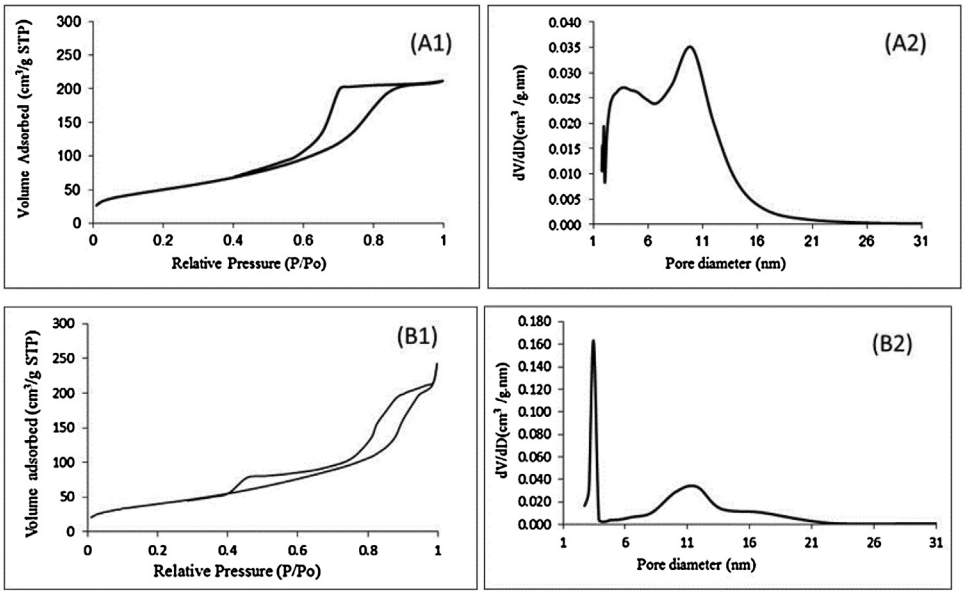

Figure 14 Adsorption isotherms (A1 and B1) and pore size distributions (A2 and B2) for calcined solids at 600 °C and 1000 °C, AS-1; AS-2 respectively.

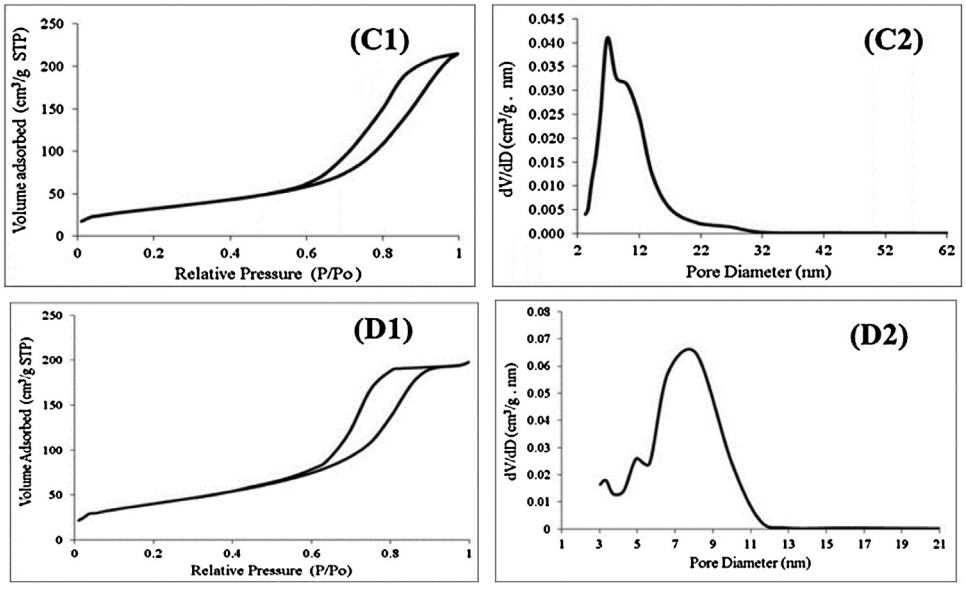

Figure 15 Adsorption isotherms (C1 and D1) and pore size distributions (C2 and D2) for calcined solids B-600, ABS-600, respectively.

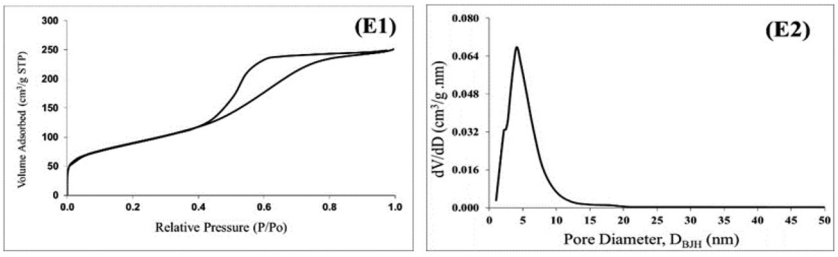

Figure 16 Adsorption isotherms (E1) and pore size distributions (E2) for calcined AG-1.

Table 3 Textural properties of calcined solids.

Precursor	Sample No	Temperature °C	S_{BET} (m^2/g)	Dp (nm)
Isopropoxide	AS-1	600	183	6.2
aluminum/stevia	AS-2	1000	148	6.8
Boehmite gel/stevia	ABS-600	600	147	9.4
Boehmite	AB-600	600	118	7.0
Glucose	AG-1	600	314	5.5

to mesoporous solids. Appreciate additionally, an H2-type hysteresis, suggesting the presence of a pore structure with interconnected channels (De Boer, 1958; Gregg & Sing, 1991; Harkins & Jura, 1943; Tilley & Eggleton, 1996; Shana et al., 2003). The isotherm B1, corresponding to the solid treated at 1000 °C, showed a similar pattern of behavior but with a major modification of its hysteresis opening and a displacement at high pressures. This is attributed to the collapse of the porous structure by the temperature effect. On the other hand, Table 3 shows the observed changes in the surface area attributed to the sintering effects, as a result of the applied heat treatment. It should be noted that despite this decrease of only 41% obtained, it is of great significance for industrial applications in the area of catalysis. Similarly, In Fig. 16, corresponding to the synthesized sample with glucose template, the isotherm described behavior type IV (IUPAC classification), evidenced the formation of mesoporosity and monomodal distribution with narrow mesopore size centered around 5.2 nm (*d* according to the BJH model). Comparatively, notable differences are observed with respect to the bi-modal character obtained for the sample synthesized with the extracts

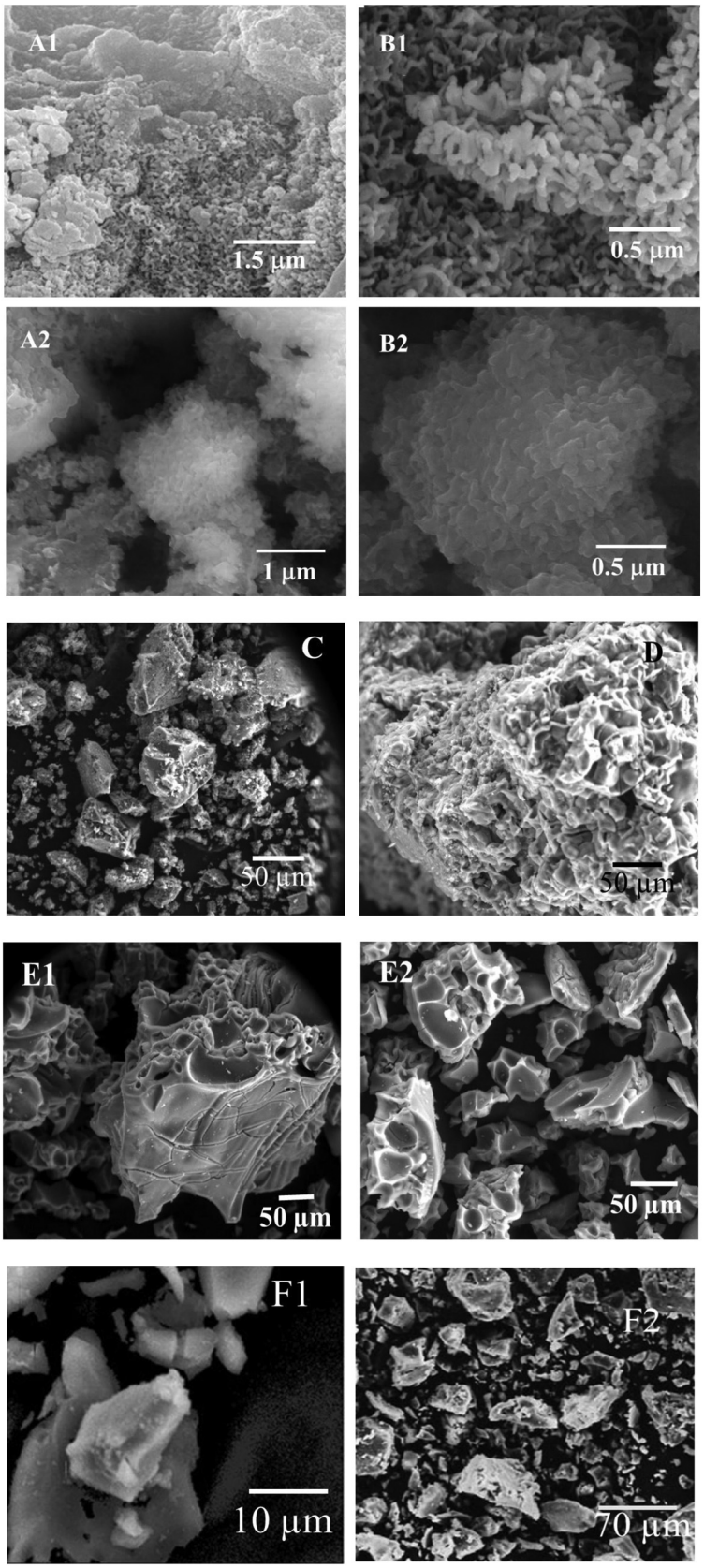

Figure 17 Micrographs (FE-SEM) of synthesized aluminas at 600 °C (A1 and B1) and 1000 °C (A2 and B2); micrographs (FE-SEM) of synthesized alumina in absence of biological template, calcinated at 600 °C (C and D); micrographs (FE-SEM) of synthesized alumina using sol–gel method and *Stevia rebaudiana* as a biological template, calcinated at 600 °C (E1 and E2); micrographs (FE-SEM) of synthesized aluminas with glucose as template (600 °C) (F1 and F2).

prepared from dried Stevia rebaudiana leaves. This can clearly be attributed to the large structural differences of both biological templates, glycosides and monosaccharides. The glycosides, molecules which contains a carbohydrate linked to another compound (a carbohydrate or an aglycon) via a glycosidic bond, are obtained when monosaccharide reacts with an alcohol in the presence of an acid catalyst. In general, the glycosides may be hydrolyzed back to their alcohol and sugar components by aqueous acid (synthesis extract) (Rodríguez, Sifontes, Méndez, Díaz, et al., 2013). However, the stability of steviol glycosides under pH conditions ranging from 2 to 10 and at temperatures of up to 120 °C, favoring the performance and use as a biological template. On the other hand, competitively, the sugar acids, such as D-gluconic, polyhydroxy dicarboxylic acids $HO_2C(CHOH)nCO_2H$, that are formally produced by oxidation of aldoses (glucose), are a mild organic acid with good chelation properties, what would happen to the formation of a hybrid compound (organic–inorganic), intermediate precursor to achieve the final product, the aluminum oxide (Calderón & Fragachán, 2007) In Fig. 17(A1, B1; A2, B2), The micrographs (FE-SEM) of calcined aluminas AS1 and AS2 are presented. In Figures A1 and B1, the grains of the solid obtained at 600 °C present a tubular morphology, as nanorods and with dimensions that are located in the nanometric scale (40–120 nm). The micrographs A2 and B2 of Fig. 17, corresponding to the calcined solid at 1000 °C, show that there were no significant changes in the morphology of the synthesized material, but the presence of aggregates of nanoparticles whose order of magnitude reaches 180–260 nm may be clearly noticed.

Differently, in micrographs 17C and 17D, corresponding to a synthesized solid in the absence of the biological template, particles of irregular morphology and a wide range of particle sizes were observed. In Fig. 17(E1 and E2), micrographs corresponding to the alumina synthesized using a sol gel method, the obtaining of particles of large sizes (>50 μm) can be appreciated, characteristic which make it unsuitable for use as a catalytic support. The 17F1 and 17F2 micrographs correspond to the synthesized aluminas using the glucose template can be observed that all the powder fractions have irregular morphology and different particle sizes in the size range of 1–200 μm. Differently, aggregate formation were not detected.

Aluminas synthesized with the different biological templates at different aging times are further characterized by NH_3-TPD. Fig. 18, shows the NH_3-TPD profiles of alumina powders; quantitative results obtained for the same are summarized in Table 4. It is evident from Table 4 that the amount of ammonia desorbed from the alumina powders is higher (~0.994 mmol/g) when the sample is synthesized with glucose at short periods of aging, than that of 0.786 mmol/g observed from aluminas obtained with stevia. This amount gradually decreases with the increase in aging time, due possibly to increasing organic groups present at the surface. However, the γ-alumina powder derived from the boehmite sample, gave a lower value for the desorbed ammonia, ~0.485 mmol/g.

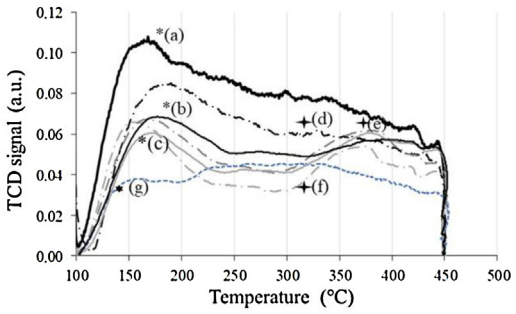

Figure 18 NH_3-TPD of aluminas obtained from isopropoxide aluminum/glucose (*(a), Isopropoxide aluminum/glucose 18 h (*(b), Isopropoxide aluminum/glucose 48 h (*(c), Isopropoxide aluminum/stevia 6 h ((d), Isopropoxide aluminum/stevia 18 h ((e), Isopropoxide aluminum/stevia 48 h ((f), boehmite gel/stevia, aging 48 h (g).

Usually, desorption peaks at 120–250 °C, 250–350 °C and 350–450 °C should be attributed to the weak, medium and strong acidic centers respectively (Chen et al., 1992). Hence, it can be inferred that the acidic sites in all aluminas are weak–strong ones. The alumina powders showed two intense peaks in the range of 100–500 °C. The first peak (I) corresponds to acidic sites attributable to the removal of adsorbed NH_3 on the solid surface. The second peak (II) is due to the slow dehydroxylation process (Chen et al., 1992) of surface hydroxyl groups on Al_2O_3. The intensity of the peaks is found to increase significantly by decreasing of the aging period during preparation. From these results, is also concluded that the alumina powder reported in the present study possesses more surface acidic sites as compared to the alumina powder obtained with the sol–gel method. The

Table 4 Summary of acidic sites measured by NH_3-TPD on calcined aluminas versus aging times.

Precursor	Sample	Temperature °C	aging time (h)	Acidic sites (mmol/g)
Boehmite sol–gel/stevia	ABS-600	600	48	0.485
Isopropoxide aluminum/stevia	AS-4	600	6	0.786
Isopropoxide aluminum/stevia	AS-3	600	18	0.722
Isopropoxide aluminum/stevia	AS-1	600	48	0.664
Isopropoxide aluminum/glucose	AG-3	600	6	0.994
Isopropoxide aluminum/glucose	AG-2	600	18	0.768
Isopropoxide aluminum/glucose	AG-1	600	48	0.702

acidities obtained through the use of the biological templates glucose and stevia presents differences, which are more notories to short periods of aging (see Table 4). Aluminas prepared with glucose always shown trend at greater acidity.

Conclusions

The richness of many molecular structures presents in the plant extracts of the *Stevia rebaudiana* open a great perspective for their extraction and their applications to the industrial sector, a most favorable application is their use in the synthesis of porous aluminas, by making likely the development of a simple preparation method through an aqueous system.

Similar results reported for aluminas prepared with glucose were obtained using the glycosides of steviol through the application of different conditions of temperature, time of aging and procedure types. They show thermal stability (600–1000 °C) and high surface areas (183–148 m^2/g), which are required properties for their application in heterogeneous catalysis.

Studies by FE-SEM demonstrated that the synthesized materials with stevia have aggregate grains with sizes in the order of 40–120 nm for the calcined solid at 600 °C and 180–260 nm for those obtained at 1000 °C. Aggregates or clusters of nanoparticles ranging from 0.5 to 10 μm were identified.

SEM measurements confirmed an average particle size in the range from 1 to 200 μm for aluminas prepared with glucose, aggregates were not detected.

FTIR studies furnished evidence for the superficial modification of aluminum oxide by carboxylate groups produced by hydrolysis of diterpenic glycosides.

The TGA profiles indicated appreciable differences between samples prepared with the two biological templates. Samples synthesized with stevia reached yields of up to 62%, while those for with glucose reached yields of 30%. The application of the sol–gel method for the biosynthesis with stevia does not favor the production of nanoscale aluminas.

Additionally, we conclude that the alumina powders reported in the present study have higher surface acidic sites.

The acidity obtained for the different aluminas synthesized by the use of biological templates follow the trend: glucose > stevia > sol–gel method/stevia, in the range 0.994–0.485 mmol/g. These differences are more notorious to short periods of aging.

The applications of prolonged aging periods favor the production of η-alumina vs γ-alumina in the systems in which estevia is used, while aluminas prepared with glucose are not affected by the increase of the aging period.

All materials prepared by the proposed synthesis methods shows potential applications as supports in the field of heterogeneous catalysis.

Conflicts of interest

The authors declare no conflicts of interest.

Acknowledgments

The authors thank *Lic. Liz Cubillán* and MSc. *Edgar Cañizales* for the assistance provided, respectively, in the FTIR and FE-SEM studies; Electronic Microscopy Unit-IVIC. The Venezuelan Institute of Scientific Research IVIC for financial support through the PROJECT 1327. *Lic. Antonio Ricardo and Lic. Salvador García*, PDVSA-Intevep. Laboratory of thermal analysis and chemisorption of the departmental management of strategic research in refining.

We thank *Prof. Dr. Jean Pasquali Zanin* for his advice and excellent suggestions.

References

Akhtar, S., Panwar, J., & Yun, Y. (2013). Biogenic synthesis of metallic nanoparticles by plant extracts. *ACS Sustainable Chemistry & Engineering*, *1*(6), 591–602.

Baltrusaitis, J., Jensen, J. H., & Grassian, V. (2006). FTIR spectroscopy combined with isotope labeling and quantum chemical calculations to investigate adsorbed bicarbonate formation following reaction of carbon dioxide with surface hydroxyl groups on Fe_2O_3 and Al_2O_3. *Journal of Physical Chemistry B*, *110*(24), 12005–12016.

Barron, A. (2014). The interaction of carboxylic acids with aluminum oxides: Journeying from a basic understanding of alumina nanoparticles to water treatment for industrial and humanitarian applications. *Dalton Transactions*, *43*(22), 8127–8143.

Bendig, L., & Scamehorn, J. (1978). Method for producing bayerite. In *United States Patent 4*. pp. 106–117.

Brinker, C., & Scherer, G. (1990). *Sol–gel science: The physics and chemistry of sol–gel processing*. Academic Press: New York.

Brunauer, S., Emmett, C., & Teller, E. (1938). Adsorption of gases in multimolecular layers. *Journal of the American Chemical Society*, *60*(2), 309–319.

Bujak, T., Nizioł-Łukaszewska, Z., Gaweł-Bęben, K., Seweryn, A., Kucharek, M., Rybczyńska-Tkaczyk, K., et al. (2015). The application of different Stevia rebaudiana leaf extracts in the ''green synthesis'' of AgNPs''. *Green Chemistry Letters and Review*, *8*(3–4), 78–87.

Burkin, A. R. (1987). *Production of aluminum and alumina: Critical reports on applied chemistry*. pp. 12–16. John Wiley & Sons: New York.

Calderón, J. A., & Fragachán, G. (2007). Preparation of mesoporous aluminas using microwave technology. In *Thesis to obtain chemical engineering degree*. Central University of Venezuela.

Chen, F. R., Davis, J. G., & Fripiat, J. (1992). Aluminum coordination and lewis acidity in transition aluminas. *Journal of Catalysis*, *133*(2), 263–278.

Davison, K. B. (1965). Organic aluminum compounds. In *United States Patents, US3173934A*.

De Boer, J. H. (1958). In D. H. Everett, & F. S. Stone (Eds.), *The structure and properties of porous materials*. London: Butterworth.

Digne, M., Sautet, P., Raybaud, P., Toulhoat, H., & Artacho, E. (2002). Structure and stability of aluminum hydroxides: A theoretical study. *Journal of Physical Chemistry B*, *106*(20), 5155–5162.

Donald, E. K. (2000). Nitric acid removal from oxidation products. In *United States Patent, 6049004*.

Galhotra, P. (2010). *Carbon dioxide adsorption on nanomaterials, Ph.D. Thesis (Doctor of Philosophy)*. University of Iowa.

Golinska, P., Wypij, M., Ingle, A. P., Gupta, I., Dahm, H., & Rai, M. (2014). Biomedical applications and cytotoxicity. *Applied Microbiology and Biotechnology*, *98*(19), 8083–8097.

Gregg, S., & Sing, K. (1991). *Adsorption surface area and porosity*. Academic Press: London.

Harkins, W. D., & Jura, G. (1943). Surface of solids XII: An absolute method for the determination of the area of a finely divided crystalline powder. *Journal of Chemical Physics*, *66*(8), 1366–1373.

Haworth, W. N., & Jones, W. G. M. (1944). Some derivatives of glucosaccharic acid. *Journal of the Chemical Society*, 66–67.

Hoggan, P., Bensitel, M., & Lavalley, J. (1994). A new method of calculating interactions between adsorbates and metal-oxide surfaces: Application to the study of CO_2 insertion in hydroxyl or methoxy groups on Al_2O_3 and TiO_2. *Journal of Molecular Structure*, *320*, 49–56.

Iordan, A., Zaki, M., & Kappenstein, C. (2004). Formation of carboxy species at CO/Al_2O_3 interfaces: Impacts of surface hydroxylation, potassium alkalization and hydrogenation as assessed by in situ FTIR spectroscopy. *Physical Chemistry Chemical Physics*, *6*(9), 2502–2512.

John, C. S., Alma, N. C. M., & Hays, G. R. (1983). Characterization of transitional alumina by solid-state magic angle spinning aluminum NMR. *Applied Catalysis*, *6*(3), 341–546.

Khaleel, A., & Klabunde, K. (2002). Characterization of aerogel prepared high-surface-area alumina: In situ ftir study of dehydroxylation and pyridine adsorption. *Chemistry*, *8*(17), 3991–3998.

Kim, S. M., Lee, Y., Bae, J., Potdar, H. S., & Jun, K. (2008). Synthesis and characterization of a highly active alumina catalyst for methanol dehydration to dimethyl ether. *Applied Catalysis A*, *348*(1), 113–120.

Kim, Y., Kim, C., Kim, P., & Yi, J. (2005). Effect of preparation conditions on the phase transformation of mesoporous alumina. *Journal of Non-Crystalline Solids*, *351*(6), 550–556.

Komarneni, S., Roy, R., Fyfe, C. A., & Kennedy, G. J. (1985). Preliminary characterization of gel precursors and their high-temperature products by ^{27}Al magic-angle spinning NMR. *Journal of the American Ceramic Society*, *68*(9), 243–245.

Kroyer, G. (2010). Stevioside and stevia-sweetener in food: Application, stability and interaction with food ingredients. *Journal für Verbraucherschutz und Lebensmittelsicherheit*, *5*(2), 225–229.

Langle, A., González, M., Carmona, G., Moreno, J., Venegas, B., Muñoz, G., et al. (2015). Stevia rebaudiana loaded titanium oxide nanomaterials as an antidiabetic agent in rats. *Revista Brasileira de Farmacognosia*, *25*(2), 145–151.

Lippens, B. C., & Boer, H. (1964). Study of phase transformations during calcination of aluminum hydroxides by selected area electron diffraction. *Acta Crystallographica*, *17*(10), 1312–1321.

Liu, Q., Wang, A., Wang, X., & Zhang, T. (2006). Mesoporous-alumina synthesized by hydro-carboxylic acid as structure-directing agent. *Microporous and Mesoporous Materials*, *92*(1–3), 10–21.

Livage, J., Henry, M., & Sanchez, C. (1988). Sol–Gel chemistry of transition metal oxides. *Progress in Solid State Chemistry*, *18*(4), 259–341.

Maciver, D. S., Tobin, H. H., & Barth, R. (1963). Catalytic aluminas. I. Surface chemistry of eta and gamma alumina. *Journal of Catalysis*, *2*(6), 485–497.

Maciver, D. S., Wilmot, W. H., & Bridges, J. M. (1964). Catalytic aluminas. II. Catalytic properties of eta and gamma alumina. *Journal of Catalysis*, *3*(6), 502–511.

Márquez, C., González, V., Díaz, I., Grande, M., Blasco, T., & Pérez, J. (2005). Sol–gel synthesis of mesostructured aluminas from chemically modified aluminum sec-butoxide using non-ionic surfactant templating. *Microporous and Mesoporous Materials*, *80*(1), 173–182.

Martín, E., & Weaver, M. (1993). Synthesis and properties of high purity alumina. *American Ceramic Society Bulletin*, *72*(7), 71–76.

Meinhold, R. H., Slade, R. C. T., & Newman, R. H. (1993). High field MAS NMR, with simulations of the effects of disorder on lineshape, applied to thermal transformations of alumina hydrates. *Applied Magnetic Resonance*, *4*(1–2), 121–140.

Mishra, D., Anand, S., Panda, R. K., & Das, R. P. (2000). Hydrothermal preparation and characterization of boehmites. *Materials Letters*, *42*(1), 38–45.

Mizushima, Y., Hori, M., & Sasaki, M. (1993). ^{27}Al MAS-NMR spectra of alumina aerogels. *Journal of Materials Research*, *8*(9), 2109–2111.

Morterra, C., Zecchina, A., Coluccia, S., & Chiorino, A. (1977). IR spectroscopic study of CO_2 adsorption onto eta-Al_2O_3. *Journal of the Chemical Society, Faraday Transactions I*, *73*, 1544–1560.

Muller, D., Gessner, W., Samoson, W., Lippma, E., & Scheler, G. (1986). Solid-state aluminum nuclear magnetic resonance chemical shift and quadrupole coupling data for condensed AlO_4 tetrahedra. *Journal of the Chemical Society, Dalton Transactions*, *6*, 1277–1281.

Niesz, K., Yang, P., & Somorjai, G. A. (2005). Sol–gel synthesis of ordered mesoporous alumina. *Chemical Communications*, *15*, 1986–1987.

Panasyuk, G. P., Azarova, L. A., Voroshilov, I. L., & Demina, L. I. (2011). Preparation of nanocrystalline aluminum hydroxide and alumina by thermal and vapor heat treatments of reaction products of terephthalic acid and aluminum hydroxide. *Inorganic Materials*, *47*(3), 273–278.

Park, Y. K., Tadd, E. H., Zubris, M., & Tannenbaum, R. (2005). Size-controlled synthesis of alumina nanoparticles from aluminum alkoxides. *Materials Research Bulletin*, *40*(9), 1506–1512.

Pecharromán, C., Sobrados, I., Iglesias, J., Gonzalez, T., & Sanz, J. (1999). Thermal evolution of transitional aluminas followed by nmr and ir spectroscopies. *Journal of Physical Chemistry B*, *103*(30), 6160–6170.

Pinnavaia, T. J., Zhang, Z., & Hick, R. (2003). Mesostructured transition aluminas. In *United States Patents, US7090824B2*.

Prakash, I., Gil, M., Bunders, C., Romila, D., Ramirez, C., Devkota, K. P., et al. (2017). A novel diterpene glycoside with nine glucose units from *Stevia rebaudiana bertoni*. *Biomolecules*, *7*(1), 1–10.

Ramis, G., Busca, G., & Lorenzelli, V. (1991). Low-temperature CO_2 adsorption on metal oxides. Spectroscopic characterization of some weakly adsorbed species. *Materials Chemistry and Physics*, *29*(1–4), 425–435.

Raybaud, P., Dignea, M., Iftimie, R., Wellens, W., Euzen, P., & Toulhoat, H. (2001). Morphology and surface properties of boehmite (γ-AlOOH): A density functional theory study. *Journal of Catalysis*, *201*(2), 236–246.

Rodríguez, M., Sifontes, Á., Méndez, F., Díaz, Y., Cañizales, E., & Brito, J. (2013). Template synthesis and characterization of mesoporous γ-Al_2O_3 hollow nanorods using stevia rebaudiana leaf aqueous extract. *Ceramics International*, *39*(4), 4499–4506.

Rodríguez, M., Sifontes, A. B., Méndez, F. J., Cañizalez, E., Mónaco, A., Tosta, M., et al. (2013). Synthesis and characterization of anatase TiO_2 nanofibers using stevia rebaudiana leaf aqueous extract. In A. Gayathri (Ed.), *Recent Res. Devel. Mat. Sci.* (Vol. 10) (pp. 45–58). Research Singpost. ISBN: 978-81-308-0518-4.

Sabari, V., Sarathi, R., Chakravarthy, S. R., & Venkataseshaiah, C. (2004). Studies on production and characterization of nano-Al_2O_3 powder using wire explosion technique. *Materials Letters*, *58*(6), 1047–1050.

Sadeghi, B., Mohammadzadeh, M., & Babakhani, B. (2015). Green synthesis of gold nanoparticles using stevia rebadiauna leaf extracts: Characterization and their stability. *Journal of Photochemistry and Photobiology B*, *148*, 101–106.

Schilling, C. H., Sikora, M., Tomasik, P., Li, Ch., & García, V. (2002). Rheology of alumina-nanoparticle suspensions: Effects of lower saccharides and sugar alcohols. *Journal of the European Ceramic Society*, *22*(6), 917–921.

Shana, Z., Jansen, J., Zhoub, W., & Maschmeye, T. H. (2003). Al-TUD-1: Stable mesoporous aluminas with high surface areas. *Applied Catalysis A*, *254*(2), 339–343.

Shek, H., Lai, J., Gu, T. S., & Lin, G. (1997). Transformation evolution and infrared absorption spectra of amorphous and crystalline nano-Al_2O_3 powders. *Nanostructured Materials*, *8*(5), 605–610.

Shirai, T., Watanabe, H., Fuji, M., & Takahashi, M. (2009). Structural properties and surface characteristics on aluminum oxide powders. *Ceramic Foundation Engineering Research Center Annual Report*, *9*, 23–31.

Sifontes, A. B., Ávila, E., Cañizales, E., Rondón, W., Gutiérrez, B., Méndez, F., et al. (2015). *Ent*-kaurane diterpenoid glycosides as soft-templates for the synthesis of high-surface area anatase titanium dioxide. An electron microscopy Study and rietveld refinement. *Biointerface Research in Applied Chemistry*, *5*(1), 5903–5909, 2069-5837.

Sifontes, A. B., Rodríguez, M., Freire, D., Rondón, W., Llovera, L., Cañizales, E., et al. (2013). Biological template based on ent-kaurane diterpenoid glycosides for the synthesis of inorganic porous materials. *Advances in Chemical Engineering and Science*, *3*(4), 278–285.

Souza, P., Souza, H., & Toledo, S. P. (2000). Standard transition aluminas. Electron microscopy Studies. *Materials Research*, *3*(4), 104–114.

Stanek, M., Kocourek, C. J., & Pacak, J. (1963). *The monosaccharides*. pp. 744. New York: Academic Press.

Tilley, D., & Eggleton, R. (1996). The natural occurrence of eta-alumina (η-Al_2O_3) in bauxite. *Clays and Clay Minerals*, *44*(5), 658–664.

Tonkovic, M., & Bilinski, H. (1994). Glucose and glucuronic acid interactions with hydrolyzed aluminum (III). *Polyhedron*, *14*(8), 1025–1030.

Toro, P., Beltran, A., Beltran, D., Cabrera, S., El Haskouri, J. M., & Martínez, M. D. (2001). Method for preparing mixed porous oxides materials thus obtained and the uses thereof. In *Patent WO2001072635 A1*.

Upreti, M., Dubois, G., & Prakash, I. (2012). Synthetic study on the relationship between structure and sweet taste properties of steviol glycosides. *Molecules*, *17*(4), 4186–4196.

Urretavizcaya, G., Cavalieri, A. L., Porto, J. M., & Sanz, J. (1998). The thermal evolution of alumina prepared by the sol–gel technique. *Journal of Materials Synthesis and Processing*, *6*, 1–7. ISSN: 1064-7562.

Xiao, T., Xu, B., Yan, Z., Sun, X., Sloan, J., González-Cortés, S., et al. (2006). Synthesis of mesoporous alumina with highly thermal stability using glucose template in aqueous system. *Microporous and Mesoporous Materials*, *91*, 293–295.

Yoldas, B. (1973). Hydrolysis of aluminum alkoxides and bayerite conversion. *Journal of Chemical Technology & Biotechnology*, *23*, 803–809.

Yoldas, B. E. (1975). Alumina sol preparation from alkoxides. *American Ceramic Society Bulletin*, *54*(3), 289–291.

Yúnes, S. (2000). *El uso de diferentes técnicas en la caracterización textural de los sólidos. adsorción de gases y porosimetría de mercurio Taller de Caracterizaciones Básicas de Materiales Catalíticos y Adsorbentes. Facultad de Ciencias*. pp. 52–64. Mérida: Universidad de Los Andes.

Zhou, R., & Snyder, R. (1991). Structures and transformation mechanisms of the, the η, γ and θ transition aluminas. *Acta Crystallography B*, *47*, 617–630.

Zyl, A., Van Thackeray, M., Duncan, G., & Kingon, A. (1993). The synthesis of *beta*-alumina from aluminum hydroxide and oxyhidroxide precursors. *Materials Research Bulletin*, *28*(2), 145–147.